

Showcasing research from the group of Prof. Vito Rizzi, University of Bari "Aldo Moro", Department of Chemistry, Italy.

Kiwi peel waste as a recyclable adsorbent to remove textile dyes from water: Direct Blue 78 removal and recovery

This work investigates the use of kiwi peels to remove Direct Blue 78 from water, as predicted by circular bioeconomy principles. So, a food waste was proposed as a recyclable adsorbent substrate, and the adsorption process was thus fully characterized, investigating the roles of ionic strength, pH values, adsorbent/pollutant amounts, and temperature. The results offered the possibility to recycle both the dye and kiwi peels and dyeing experiments were also attempted.

As featured in:



See Vito Rizzi *et al.*,  
*Phys. Chem. Chem. Phys.*,  
2024, **26**, 9891.



Cite this: *Phys. Chem. Chem. Phys.*,  
2024, 26, 9891

# Kiwi peel waste as a recyclable adsorbent to remove textile dyes from water: Direct Blue 78 removal and recovery†

Jennifer Gubitosa,<sup>a</sup> Vito Rizzi,<sup>a</sup>  \*<sup>a</sup> Paola Fini,<sup>b</sup> Sergio Nuzzo<sup>b</sup> and  
Pinalysa Cosma <sup>ab</sup>

According to circular bioeconomy principles, the use of kiwi peels to remove Direct Blue 78 (DB) from water is investigated during this work, proposing food waste as a recyclable adsorbent substrate. Direct Blue 78 (DB) was adopted as a model pollutant, employing its visible spectrum to monitor its adsorption. The adsorption process was thus fully characterized, investigating the roles of ionic strength, pH values, adsorbent/pollutant amounts, and temperature. The thermodynamics, kinetics, and adsorption isotherms were also studied. To extend the kiwi peels' lifetime, quite complete desorption was obtained by adopting hot water as a safe and eco-friendly strategy. Despite the relatively low kiwi peels' maximum adsorption capacity ( $6 \text{ mg g}^{-1}$ ) for DB when adsorbed in the presence of NaCl, 10 cycles of adsorption/desorption were attempted, proposing the recycling of both the dye and kiwi peels as dictated by circular economy principles. Dyeing experiments were also performed, evidencing the dye's ability to color cotton fabrics after its recycling. Finally, the removal of other textile dyes, Direct Red 83:1 and Direct Yellow 86, was demonstrated in a mixture with DB. A preliminary investigation was performed to find the best working conditions for inducing the solid-state dye photodegradation, proposing a possible alternative for the adsorbent regeneration.

Received 15th January 2024,  
Accepted 23rd February 2024

DOI: 10.1039/d4cp00174e

rsc.li/pccp

## Introduction

Environmental disorders and pollution have become important worldwide issues for several years, and research activities in this context are still very active.<sup>1–17</sup> Among different classes of pollutants, dyestuffs constitute an important concern because they are toxic and dangerous for human health and aquatic living systems, inducing several diseases.<sup>2,9,11–15</sup> Currently, more than 100 000 dye types are available on the market, and more than  $7 \times 10^5$  tons are generated every year. So, their presence in water effluents is attained.<sup>18</sup> However, dyes are not biodegradable and are very stable substances, resistant to light irradiation and heat. The degradation by using oxidizing agents cannot be considered a powerful tool due to their resistance, and, in any case, hard working conditions are needed.<sup>11,12,18</sup> It is worth mentioning that, among textile dyes, azo dyes are extensively used and account for 70% of the total dye

production.<sup>18</sup> Due to the toxicity of amine groups in their chemical structure, azo dyes are considered hazardous compounds for the whole environment.<sup>11,12,18</sup> Due to the large color production from industries, innovative and performant ways to remove these dyes efficiently from water should be developed, with particular attention to methods that agree with green chemistry principles, sustainability, and bioeconomy concepts.<sup>19</sup> Several advantages arise. For this purpose, among the possible strategies used for the dye's removal (such as ion exchange, coprecipitation, filtration, reverse osmosis, Fenton oxidation, photodegradation, biodegradation, ozonation, and electrochemical reduction), the adsorption methodologies have been extensively studied for water remediation.<sup>11,12,18,20–32</sup> Indeed, adsorption is considered a low-cost approach that should avoid the release of secondary by-products as could occur, for example, when advanced oxidation processes are used.<sup>16</sup> Furthermore, the adsorption could be easily implemented from the laboratory to industrial scale.

Due to the necessity of developing greener technologies, the innovative tendency represented by the use of wastes as adsorbent materials to remove pollutants from water has been increasing in the last few years. Particularly, the use of fruit wastes is well known, and the work of Bhatnagar *et al.*<sup>33</sup> is very interesting for showing, among wastes, the use of fruit and

<sup>a</sup> Dipartimento di Chimica, Università degli Studi di Bari "Aldo Moro",  
Via Orabona, 4-70126 Bari, Italy. E-mail: vito.rizzi@uniba.it

<sup>b</sup> Consiglio Nazionale delle Ricerche CNR-IPCF, UOS Bari, Via Orabona,  
4-70126 Bari, Italy

† Electronic supplementary information (ESI) available. See DOI: <https://doi.org/10.1039/d4cp00174e>

vegetable peels for the removal of pollutants. Indeed, most fruit peels become waste without applications, with potential problems for their management. So, to face this problem, a policy is being implemented to ensure sustainable production and consumption models to achieve very important targets for the transition from linear to circular models, giving waste a new life.<sup>34</sup> On this ground, this work proposes a sustainable management, efficient use of natural resources as dictated by bioeconomic principles, and reduction of waste through recycling to meet the requirements of the circular bioeconomy.<sup>19</sup> An upcycling process of existing materials is thus presented, following the new eco-centric trend, valorizing the use of food wastes, particularly kiwi peels, as recyclable adsorbent materials for dye removal. Indeed, some authors of this paper recently have reported the use of this waste/adsorbent for the removal of emerging pollutants, presenting for the first time the chemical and physical features of kiwi peels.<sup>34,35</sup> In particular, Gubitosa *et al.*,<sup>34,35</sup> by the synergistic use of different techniques (such as SEM investigation, FTIR-ATR, and TG analyses), showed that the adsorbent is characterized by particular morphological features, irregular domains, and filaments on both sides of peels' surfaces, and it is mainly constituted by lignin, cellulose, and hemicellulose. Furthermore, it was demonstrated that the main morphological and chemical features of kiwi peels were also retained after their use and reuse during the adsorption/desorption processes, enabling kiwi peels as a long-lasting adsorbent material.<sup>34,35</sup> This work aims to widen the kiwi peels' applicability, proposing that this waste can also be used for the anionic textile dye removal from water. Indeed, about this concern, only one work is reported in the literature, and it refers to methylene blue and rhodamine B removal.<sup>36</sup> On the other hand, kiwi peels, to our knowledge, were employed in the past to remove  $\text{Cd}^{2+}$ ,  $\text{Cr}^{3+}$  and  $\text{Zn}^{2+}$  ions,<sup>37</sup> nitrate,<sup>38</sup> and oil,<sup>39</sup> sequester  $\text{Pb}^{2+}$ ,<sup>40</sup> and, as previously said, to remove emerging pollutants.<sup>34,35</sup> Therefore, a deep scientific research activity should be developed to promote the sustainable management of kiwi peels' wastes to address environmental problems related to dye pollution. Moreover, an important aspect of this paper is related to the eco-friendly kiwi peel pre-treatment, avoiding hard experimental conditions and hazardous materials, as already reported by Gubitosa *et al.*<sup>34,35</sup>

Furthermore, the adsorbent recycling was proposed under safe conditions, demonstrating the dyestuff reuse. More specifically, kiwi peels (i) were only washed with hot water, avoiding the use of toxic chemicals, leading to the development of an eco-design in accordance with an eco-innovation model, especially for a potential future perspective to implement the process on a large-scale; (ii) hot water was used to desorb the color, regenerating the adsorbent, dyeing cotton fibers again. In detail, to highlight the main features of the proposed adsorption process, among textile dyes, an azo one, Direct Blue 78 (DB), was selected as a model anionic compound. So, the DB adsorption process has been investigated, showing the process's mechanism, related kinetics, and thermodynamic characteristics. The DB removal was observed in the presence of an acid solution (pH 2) or salts, suggesting that, during the

process, the involved interacting forces were mainly electrostatic and hydrophobic. By focusing the attention on the DB removal in the presence of salt, 10 adsorption/desorption cycles were studied, avoiding the disposal of the adsorbent as secondary hazardous waste material, recovering 90% of the DB. The adsorbent lifetime was thus extended, according to the Green Economy requests.<sup>16</sup> The maximum adsorption capacity of kiwi peels towards DB was inferred ( $q_{\text{max}} = 6 \text{ mg g}^{-1}$ ), and it well agrees with the values obtained by other natural adsorbents during the removal of anionic dyes.<sup>18,20–32</sup> However, if some of the used materials showed high adsorption capacities and performances,<sup>41,42</sup> it is worth mentioning that only a few studies<sup>26,29,30,32</sup> discussed the adsorbent regeneration, and thus the dye desorption. In particular, concentrated NaOH solutions were proposed in these studies by proposing a long contact time and low desorption efficiency, applying only a few cycles of adsorption/desorption. In contrast, in this paper, hot water is proposed for the kiwi peel regeneration, recycling both the dye and the adsorbent for 10 cycles, which could be implemented because no change in terms of kiwi peels' efficiency was observed. Furthermore, a dye mixture was also investigated, and kiwi peels were able to remove and desorb the mixtures of colors without any competitive effects. Additionally, focusing attention on DB, the recycled color was used again to dye cotton fibers, demonstrating its reuse. Finally, preliminary results related to the solid-state DB photodegradation after the adsorption were discussed as a potential alternative for the adsorbent regeneration by using advanced oxidation processes (AOPs). In particular, the use of  $\text{TiO}_2$  and UV light appeared as the best promising approach to obtain the DB degradation that occurred  $\approx 75\%$  after 8 h of irradiation time, under the proposed experimental working conditions. Novel horizons in the environmental field are thus opened, considering that this adsorbent is also able to adsorb emerging pollutants from water and desorb them in salt solutions.<sup>34,35</sup> On the other hand, the removal of color was observed in a completely reversed situation: adsorption in salt solutions and desorption in water. So, kiwi peels, compared with other adsorbents, could be potentially considered “on-demand” adsorbents, being able to remove different classes of pollutants, according to the working conditions.

## Results and discussion

### Direct Blue removal by kiwi peels

The study was carried out using visible spectroscopy as a powerful tool to rapidly monitor the amount of the anionic dye, DB, in water and consequently infer the role of parameters affecting its removal by kiwi peels' wastes. In the visible spectrum, the DB solution showed the main maximum absorption band at  $\lambda = 600 \text{ nm}$  (Fig. 1).

It can be attributed to a  $\pi-\pi^*$  transition arising from the characteristic dye chromophore, comprising azo groups ( $-\text{N}=\text{N}-$ ) interacting with the adjacent aromatic moieties.<sup>11–13</sup> This band was thus considered diagnostic to monitor the

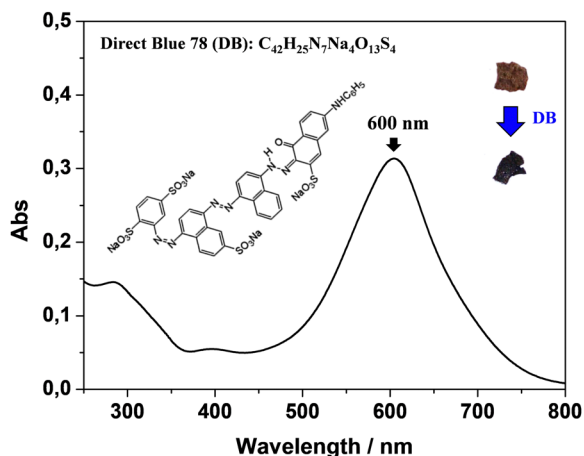


Fig. 1 Visible spectrum of a DB solution  $13 \text{ mg L}^{-1}$ , pH 6. In the inset, the chemical structure and formula of DB are reported, along with the kiwi peels that change their color from dark brown to blue after the DB adsorption.

removal of color from water. As a first step, adsorption experiments were performed at room temperature by adding 50 mg of peels in distilled water at pH 6 in the presence of  $13 \text{ mg L}^{-1}$  of DB. The lack of DB adsorption was observed.

This result could be indicative of electrostatic repulsion between negatively charged DB and the kiwi peel surface.<sup>11–13,27,34</sup> Accordingly,  $\text{pH}_{\text{PZC}}$  of the adsorbent, experimentally calculated as reported in Fig. S1 (ESI<sup>†</sup>), occurred at around pH 4. So, it means that the adsorbent surface at  $\text{pH} < 4$  and  $\text{pH} > 4$  was positively and negatively charged, respectively.<sup>34</sup> At the same time, DB's chemical features should be considered (see Fig. 1 for the DB chemical structure) to clarify the finding. The DB sulfonate groups ( $-\text{SO}_3^-$ ) were always deprotonated, having a  $\text{pK}_a < 2$ . This means that, at pH 6, DB was negatively charged, and it was repelled by the kiwi peels' surface. On the other hand, the  $\text{pK}_a$  value of the tertiary amino group is around 4, while primary and secondary amino groups start their deprotonation at pH 9.<sup>12</sup> After these assessments, to favor the DB adsorption, it was necessary to lower the solution pH value. In these conditions, the adsorbent was positively charged, and favored the attraction of the DB sulphonate groups. Alternatively, it should be possible to perturb the charges by affecting the ionic strength of the solution containing DB and the adsorbent. So, in the first step, the effect of pH on the adsorption process was investigated by using eqn (1) for calculating the % of Ads, by adopting 60 minutes as the constant contact time. Fig. 2(A) reports the obtained results. As expected, the DB removal was high at  $\text{pH} < 4$  and decreased with increasing pH values. Indeed, as can be evidenced in the inset of Fig. 1, the color of kiwi peels changed from dark brown to blue. The DB adsorption was practically absent in the range of pH 4–12. The finding confirmed the main presence of electrostatic interactions between the  $-\text{SO}_3^-$  moieties of DB and the surface of kiwi peels.<sup>12,34</sup> On the other hand, the DB remained negatively charged at higher pH values, while the peels turned their charge surface from positive to negative, favoring the repulsion.

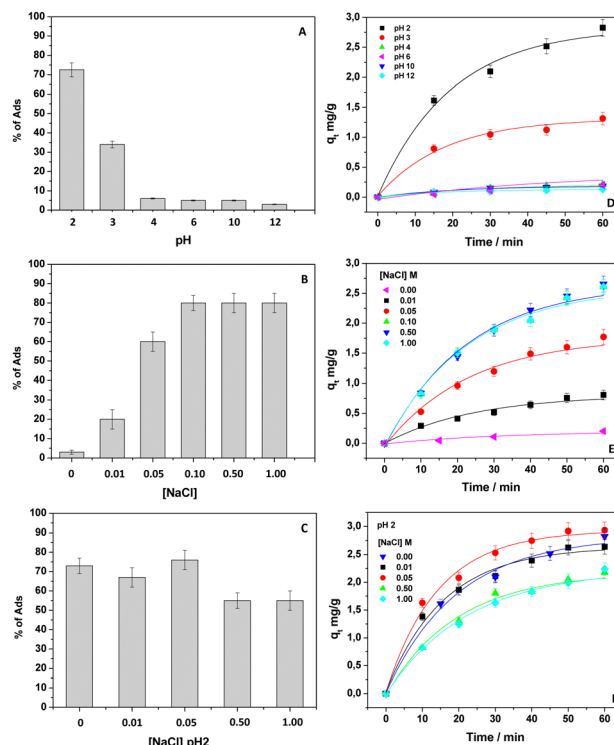


Fig. 2 % of DB adsorption onto kiwi peels at different pH values (A), NaCl concentrations at pH 6 (B), at pH 2, and different NaCl concentrations (C). Under the same conditions, the  $q_t$  values ( $\text{mg g}^{-1}$ ) at different contact times are reported (D)–(F). The experiments of DB adsorption were obtained by using DB  $13 \text{ mg L}^{-1}$  in the presence of 50 mg of kiwi peels at room temperature.

In the second step, for detailing the nature of the interaction, the % of Ads was calculated by changing the ionic strength of the solution with different salt concentrations, always adopting 60 minutes as the reference contact time. NaCl was chosen as the model electrolyte. Interesting results were obtained, as shown in Fig. 2(B). By maintaining the pH of the solution at 6 and increasing the NaCl concentration from 0.01 M to 0.1 M, the removal of DB greatly changed from 20% to 80%, and leveled off at this value. Indeed, when the salt was further increased to 0.5 and 1 M, the removal percentage was the same. The electrolyte presence partially neutralized the charges of the adsorbent surface, reducing its negative charge, and moderately favored the attraction between DB and kiwi peels. However, at the same time, the ions from the salt also shielded the DB charges; thus, hydrophobic interactions and the H-bonds formation, as already observed by Rizzi *et al.*<sup>9</sup> in a similar work, could be also taken into account. So, the mechanism of adsorption changed according to the case: if, on the one hand, under acidic conditions of work, the coulombic interactions were mainly favored, on the other hand, by increasing the ionic strength at neutral pH, the salting-out effect should be additionally promoted in favor of hydrophobic interaction, as observed elsewhere.<sup>43,44</sup> To better understand these findings, the adsorption experiments were performed at pH 2 and in the presence of NaCl (Fig. 2(C)). By diluting the



solution containing NaCl to 0.01 and 0.05 M, the obtained adsorption percentages were quite consistent with those calculated at pH 2. Surprisingly, at higher NaCl concentrations, a significant reduction of the adsorption percentage was observed if compared with the results obtained at pH 2 and the corresponding measurement in the presence of salt at pH 6. These results suggest the competitive effect of ions that hindered the formation of electrostatic interactions observed under the acidic experimental working condition.<sup>11,12,16,34</sup> In particular, possible shielding effects of charges mediated by cations/anions, both referring to DB functional groups and the adsorbent surface and competition effects between the pollutant and ions (in this case, anions), towards the positively charged adsorbent surface, should be considered.<sup>34</sup> So, Na<sup>+</sup> might shield the DB negative  $-\text{SO}_3^-$  groups, and Cl<sup>-</sup> could compete for the positive kiwi peel surface. At pH 2, the presence of salt played a negative role, and a balance of electrostatic and hydrophobic interactions was observed. Starting from these considerations and inferring more information about the adsorption process, the adsorption capacities were calculated according to eqn (2). In particular, the study was performed by monitoring the adsorption evolution of DB onto kiwi peels' surface at several contact times (Fig. 2(D)–(F)).

As the pH of the DB solution decreased or the salt (NaCl) amount increased, the  $q_t$  values increased, confirming the establishment of favorable interactions between DB and the adsorbent already at the beginning of the process, when a greater increase in the adsorption capacity was observed. Indeed, when the adsorption started, the DB removal appeared fast, in agreement with the presence of more functional groups available to adsorb DB.<sup>6,12,28,34</sup> Furthermore, a weaker DB diffusion resistance should be considered at the beginning of the process. On the other hand, extending the contact time, a plateau region was reached, indicating the attainment of an equilibrium condition where the adsorption sites were occupied by DB.<sup>6,8,34</sup> Additionally, at the end of the adsorption, the decrease in the DB concentration gradient in the solution should slow down the whole process. Moreover, Gubitosa *et al.*<sup>34</sup> reported that when the increase in  $q_t$  values appeared slower, the presence of repulsive forces between the free pollutant molecules in the solution and those adsorbed onto kiwi peels, should also be considered.

Since, as a whole, the  $q_t$  time evolution in solutions containing DB at pH 2 and/or in the presence of salts looked similar, without important differences, the attention was focused on DB adsorption in the presence of salts, avoiding the use of acidic experimental conditions. In particular, after the evaluation of the effects of other salts on the DB adsorption onto kiwi peels, NaCl 0.5 M was selected as the reference salt concentration, and other experiments were performed to give more details about the adsorption process.

#### Effect of other salts on the DB adsorption onto kiwi peels

To get insight into the DB adsorption process, the nature of both anions and cations was changed by performing adsorption experiments at pH 6. In general, by considering the

previous discussion, it was expected that cations should play a role in shielding the DB negative charge, acting also as competitors for the negative kiwi peel surfaces, while anions should not play an important role due to the signs of the involved charges of DB and kiwi peels. By choosing 0.5 M as the reference electrolyte concentration, the salt nature was first changed by fixing the anion (Cl<sup>-</sup>) and varying the nature of the cation. Specifically, the following series of cations were adopted: Li<sup>+</sup>, Na<sup>+</sup>, K<sup>+</sup>, Mg<sup>2+</sup>, and Ca<sup>2+</sup>, and Fig. S2A (ESI<sup>†</sup>) reports the obtained results. The  $q_t$  values decreased from Li<sup>+</sup> to K<sup>+</sup>. Therefore, by increasing the hydrated radius of cation ( $K^+ = 2.32 \text{ \AA}$ ,  $Na^+ = 2.76 \text{ \AA}$ , and  $Li^+ = 3.4 \text{ \AA}$ ),<sup>3</sup> the DB adsorption was favored by better neutralizing the DB charge, allowing the interaction with kiwi peels. On the other hand, by changing the cation charge from monovalent to divalent ions (Ca<sup>2+</sup> and Mg<sup>2+</sup>), the effects tended to be similar to those observed in the presence of KCl.<sup>6,8,34</sup> Probably, the result could be attributed to the small size of these cations along with their different affinity with  $-\text{SO}_3^-$  groups, if compared with monovalent ions. Subsequently, the nature of anions was changed by selecting Na<sup>+</sup> as the cation, and Fig. S2B (ESI<sup>†</sup>) shows the results. In this case, as expected, the  $q_t$  values looked like each other.

#### Effect of DB and kiwi peel amounts on the adsorption process

The role of active sites in the DB adsorption onto kiwi peels in the presence of NaCl 0.5 M at pH 6 was investigated by changing both the adsorbent and pollutant amounts. Fig. 3 reports the  $q_t$  values calculated through eqn (2), using different quantities of dry adsorbent in contact with a  $13 \text{ mg L}^{-1}$  DB solution (Fig. 3(A)), and by varying the pollutant concentration, maintaining the kiwi peel amount constant at  $50 \text{ mg}$  (Fig. 3(B)).

As the adsorbent quantity increased from 12 to  $80 \text{ mg}$ , the  $q_t$  values decreased. However, the plateau region starting point (the condition where the equilibrium occurred) was observed later by decreasing the adsorbent amount. For example, the  $q_t$  values joined the plateau region after 20 and 50 minutes when in the presence of the highest and lowest adsorbent amount, respectively. As reported by Gubitosa *et al.*,<sup>34</sup> when great amounts of adsorbent were in use, the adsorption sites were not completely saturated, restituting low  $q_t$  values although the DB removal was high. These results indicated that the site's availability favored the DB's adsorption onto kiwi peels' surface. The process was especially enhanced at the beginning of the adsorption, as shown by the rapidity of achieving the plateau region.<sup>6,12,34</sup> Instead, by reducing the adsorbent amount, the sites for DB decreased, slowing down the DB removal, and the equilibrium was reached later.

When the initial DB concentration was changed from  $50 \text{ mg L}^{-1}$  to  $8 \text{ mg L}^{-1}$ , the adsorption capacities increased (Fig. 3(B)), highlighting the importance of DB's concentration gradient, which favored the pollutant transfer from the bulk's solution to the adsorbent.<sup>12,34</sup> As described by Gubitosa *et al.*,<sup>34</sup> in the presence of a high pollutant amount, the collisions with the active free sites of the adsorbent were enhanced, favoring the adsorption. As a whole, these results suggested that the DB mass transfer and its adsorption onto the adsorbent surface

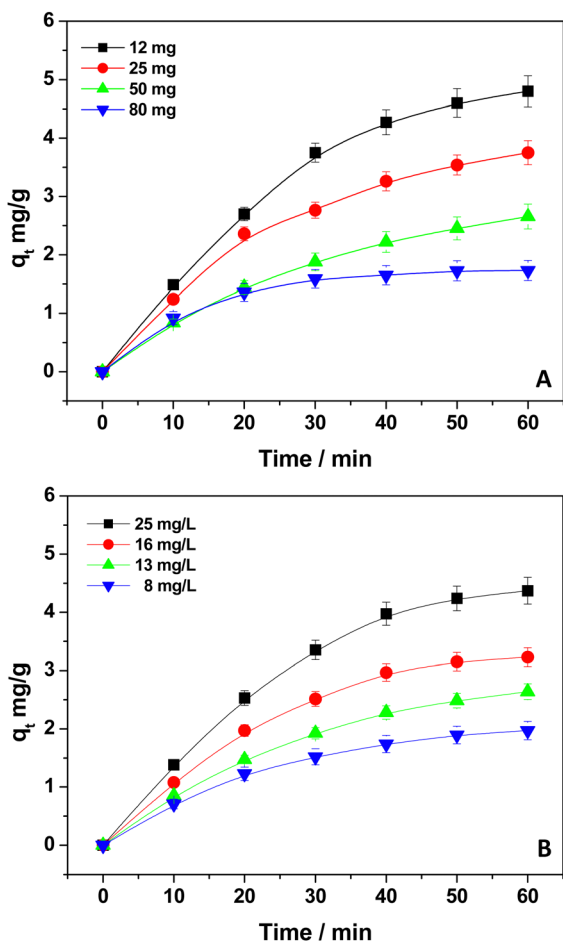


Fig. 3 Adsorption capacities  $q_t$  ( $\text{mg g}^{-1}$ ) of kiwi peels by adopting a DB solution of  $13 \text{ mg L}^{-1}$  in the presence of different adsorbent amounts (A) and by changing the DB concentrations, ranging from 25 to  $8 \text{ mg L}^{-1}$ . Experiments were performed in a NaCl  $0.5 \text{ M}$  solution by using  $50 \text{ mg}$  of kiwi peels at room temperature (B).

could have a kinetic relevance.<sup>34</sup> Once again, it should be mentioned that the equilibrium region was obtained earlier for diluted solutions; so, under these conditions, more free active sites were available and favored the DB removal, confirming their role during the process.<sup>6,8,34</sup>

### Kinetic analysis

The kinetic analysis was subsequently performed by applying both the PFO (eqn (3)) and PSO (eqn (4)) kinetic models, respectively, to the  $q_t$  values reported in Fig. 3(A) and (B). The results are shown in Fig. S3 and S4 (ESI†). In particular, Fig. S3A and S4A (ESI†) report the PSO model applied to the adsorption experiments performed by changing the DB and adsorbent amounts, respectively. Fig. S3B (ESI†) and Fig. 4(B), instead, show the PFO model under the same conditions of work. The linear fitting was thus applied to infer the corresponding kinetic parameters (Tables S1 and S2, ESI†). As suggested by the literature,<sup>6,12,31,34</sup> to choose the kinetic model suitable for describing the experimental process, the correlation coefficients  $R^2$ , and the comparison between  $q_{e,\text{exp}}$  (the experimental

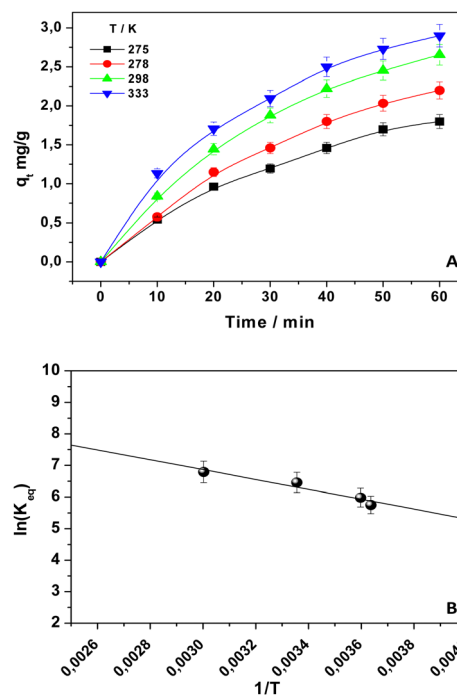


Fig. 4 Adsorption capacities  $q_t$  ( $\text{mg g}^{-1}$ ) (A) onto kiwi peels ( $50 \text{ mg}$ ) at several temperature values (from a DB solution  $13 \text{ mg L}^{-1}$ , NaCl  $0.5 \text{ M}$ , pH 6); plot of  $\ln(K_{\text{eq}})$  vs.  $1/T$  to obtain  $\Delta H^\circ$  and  $\Delta S^\circ$  at  $298 \text{ K}$  (B).

adsorption capacities at the equilibrium) and  $q_{e,\text{calc}}$  (calculated adsorption capacities, obtained by applying the kinetic equations) was considered. The analysis of the output data reported in Tables S1 and S2 (ESI†) indicated that the  $R^2$  values were acceptable for both the models, with a slightly better correlation when the PSO model was applied. Interestingly, comparing  $q_{e,\text{exp}}$  and  $q_{e,\text{calc}}$ , it is clear that the PFO model would be more suitable, even if the PSO well fitted the experimental data, restituting kinetic constants that changed with a trend according to the previous discussion. However, all these results highlighted the kinetic relevance of both the kinetic models during the DB adsorption process, suggesting the role of physisorption onto the kiwi surface (PSO), and the mass transfer of DB from the solution to the adsorbent surface (PFO) during the adsorption.<sup>34</sup> So, in the first step, the DB diffused onto the adsorbent surface (external diffusion), then it was adsorbed on the surface of kiwi peels, and later, it diffused inside (internal diffusion). Consequently, the Weber–Morris model was also applied by employing eqn (5) to assess the kinetic relevance of the intraparticle diffusion. If this model is suitable for interpreting the studied system, a straight line passing through the origin should be obtained by plotting  $q_t$  values versus  $t^{1/2}$ .<sup>28,34</sup> Once again, different amounts of adsorbent (Fig. S5A, ESI†) at constant DB concentration, and different DB concentrations in the presence of  $50 \text{ mg}$  of adsorbent (Fig. S5B, ESI†), were considered for testing the applicability of the Weber–Morris equation. As observed, the model cannot be applied in both cases since the data fitting restituted two straight lines that did not pass through the origin. So, the DB adsorption, according

to the previous discussion, involved two or more kinetic steps besides the intra-particle diffusion.<sup>28</sup> By analyzing the intraparticle diffusion results, it is possible to assess that the first straight lines described the faster DB diffusion through the boundary layer of solution to the external surface of kiwi peels. Afterward, there was the second step at the longer contact times, which described the intra-particle diffusion and adsorption as kinetic relevant steps, and at the end, the equilibrium was reached.<sup>28</sup>

### Thermodynamic analysis

The thermodynamic parameters related to the DB adsorption onto kiwi peels were inferred by changing the temperature values. Indeed, the adsorption process was studied at different temperatures, from 275 to 333 K, in solutions containing 50 mg of adsorbent and 13 mg L<sup>-1</sup> of DB at pH 6 in NaCl 0.5 M. The obtained  $q_t$  values are reported in Fig. 4(A).

By increasing the temperature values, the DB adsorption capacities increased, evidencing the endothermic character of the process.<sup>29,34</sup> In particular, the temperature effect was especially highlighted at the beginning of the adsorption process due to, once again, the presence of more free sites to host DB. So, by considering the obtained  $q_t$  values and the amount of the not adsorbed DB at equilibrium,  $K_{eq}$  was calculated for each temperature. Eqn (6) was thus applied to calculate the  $\Delta G^\circ$  values for each temperature, as reported in Table 1.

Negative  $\Delta G^\circ$  values were obtained, indicating the spontaneity of the process that occurred favored with the increase of the temperature.<sup>16,29,34</sup> By using eqn (7), *i.e.*, by plotting  $\ln(K_{eq})$  versus  $1/T$  (Fig. 4(B)), the  $\Delta H_{298}^\circ$  and  $\Delta S_{298}^\circ$  values are inferred and reported in Table 1. The high positive values of  $\Delta H_{298}^\circ > 0$  (+160 kJ mol<sup>-1</sup>) confirmed the endothermic character of the process. On the other hand,  $\Delta S_{298}^\circ > 0$  (+95 J mol<sup>-1</sup> K) suggested, as observed in other studies, that at the adsorbent-adsorbate interface, the DB adsorption increased the randomness.<sup>16,29,34</sup>

### Isotherms of adsorption

Langmuir, Freundlich, Temkin, and Dubinin-Radushkevitch (D-R) isotherm models (eqn (8)–(13)) were used to fit the experimental data.<sup>29,34</sup> Fig. 5 shows the obtained results.

The correlation factor  $R^2$ , arising from each linear fitting (Table 2), suggested the applicability of all the isotherm models, with a minor extent of the Langmuir one. In particular, the best fitting was observed with the Freundlich model ( $R^2 = 0.98199$ ). Overall, Table 2 reports the isotherm parameters calculated for each model. The results suggested that the pollutant adsorption occurred on heterogeneous surfaces, as already observed in other similar studies. Additionally, the

value of the  $n$  parameter (see Table 2), derived from the Freundlich model, represents the adsorption strength, and the values of  $1/n$  ranging from 0 to 1, as herein observed, proved that the physical DB adsorption was favored. The  $K_L$  value from the Langmuir model also supported this observation since it occurred between 0 and 1; it indicated that the adsorption was favored for the adsorbate-adsorbent system.<sup>16,29,34</sup> Finally, the D-R model was applied, and the related parameters are reported in Table 2. The small value of  $E$  highlighted the important involvement of physical forces during the DB adsorption onto the kiwi peel surface, further confirming the previous results. Indeed, the obtained value of 1 kJ mol<sup>-1</sup> was less than 8 kJ mol<sup>-1</sup>.<sup>16,29,34</sup> All these findings agreed with the calculated value of  $\Delta H_{298}^\circ$ .

### Desorption of DB and adsorbent recycling

To recycle both the adsorbent and DB, experiments of desorption were performed. The investigation occurred on kiwi peels loaded with DB adopting different experimental conditions: adsorption from an acid solution (pH 2) and from NaCl solution 0.5 M, pH 6, respectively. In detail, after the DB's adsorption (initial condition: dye concentration 13 mg and 50 mg of adsorbent), kiwi peels were left in fresh water for 15 and 60 minutes. Starting from kiwi peels loaded with DB from a solution containing NaCl, the results reported in Fig. 6(A) were observed after 60 minutes. The inset of the same figure shows the results corresponding to experiments of desorption obtained after 15 minutes of contact time. As expected, the release of DB by employing an acidic solution (pH 2) or NaCl (0.5 M) was not observed, these conditions being favorable to the dye adsorption, as discussed throughout the paper. Therefore, experimental conditions that appeared unfavorable for the DB removal will ensure the color release.

Specifically, water (pH 6) and alkaline solution (pH 12) at 298 K favored the process, further improved with the increase of temperature at 323 K, as reported in Fig. 6(A). The slight differences in terms of % of desorption between water at pH 6, and pH 12 can be better appreciated in the inset of Fig. 6(A) when a short contact time of desorption was adopted. The alkaline solution slightly favored the DB desorption, and the finding can be interpreted with the negligible presence, also in this condition, of electrostatic interactions involving an ion-exchange mechanism. A similar behavior was obtained when kiwi peels loaded with DB from an acidic solution were considered (Fig. 6(B), and the inset). In this case, according to the main electrostatic nature of the interactions between DB and the adsorbent surface, the release in water at pH 6 was not favored unless at higher temperatures. On the other hand, the use of water at pH 12 ensured the DB release at room and high temperature without important differences, confirming the role

Table 1 Thermodynamic parameters

$\Delta H_{298}^\circ$ (kJ mol <sup>-1</sup> )	$\Delta S_{298}^\circ$ (J mol <sup>-1</sup> )	$\Delta G_{275}^\circ$ (kJ mol <sup>-1</sup> )	$\Delta G_{278}^\circ$ (kJ mol <sup>-1</sup> )	$\Delta G_{298}^\circ$ (kJ mol <sup>-1</sup> )	$\Delta G_{333}^\circ$ (kJ mol <sup>-1</sup> )
+160 ± 10	+95 ± 10	-13 ± 5	-14 ± 5	-16 ± 5	-20 ± 5

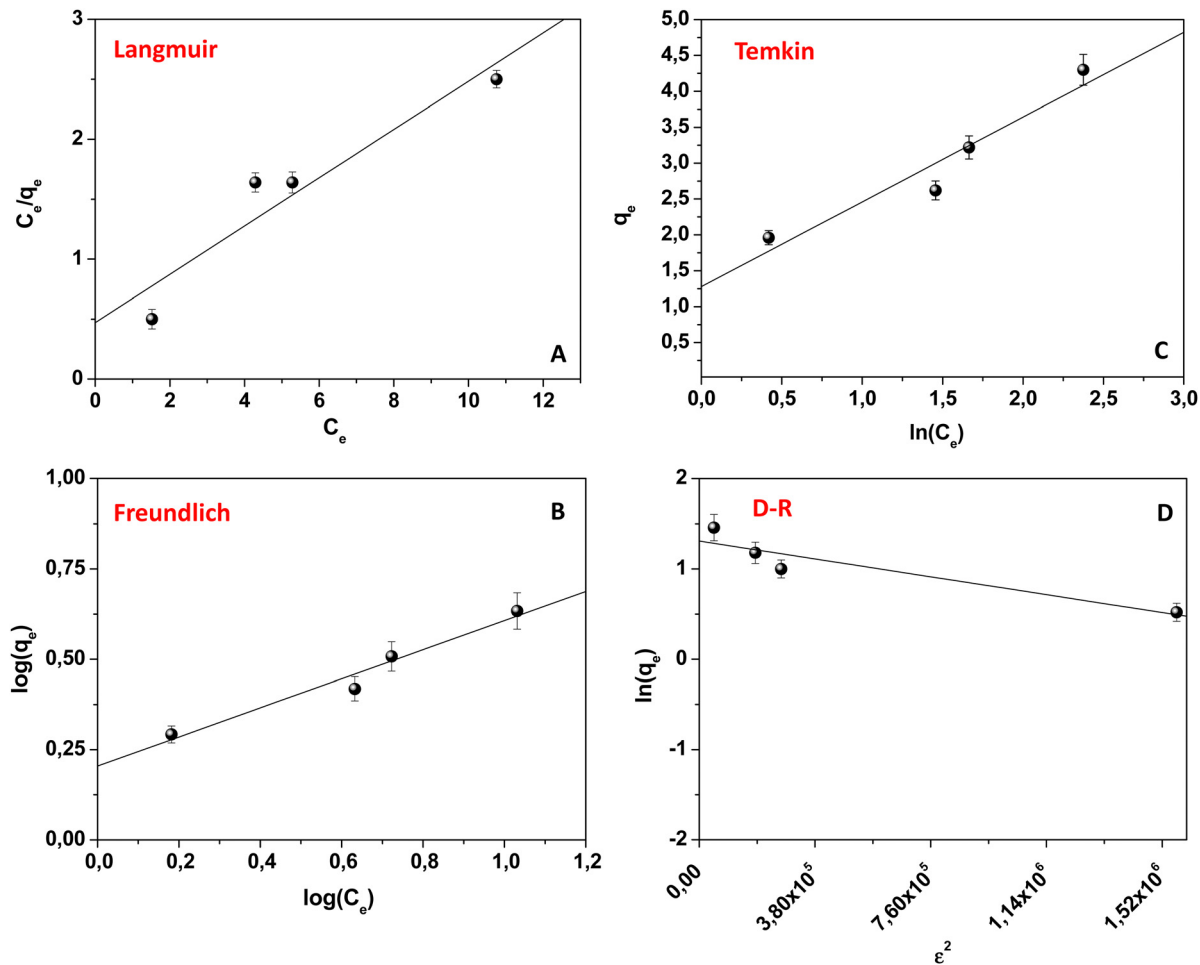


Fig. 5 Isotherms of adsorption: Langmuir (A), Freundlich (B), Temkin (C) and D–R (D).

Table 2 Isotherm parameters

Langmuir isotherm model			Temkin isotherm model		
$K_L$ (L mg <sup>−1</sup> )	$Q_0$ mg g <sup>−1</sup>	$R^2$	$K_T$ (L mol <sup>−1</sup> )	$B_1$	$R^2$
0.02	26.00	0.9493	2.85	1.20	0.96115
Freundlich isotherm model					
$K_F$ (L mg <sup>−1</sup> )	$1/n$			$R^2$	
1.60	0.40			0.98199	
D–R isotherm model					
$K_{D-R}$ (mol <sup>2</sup> J <sup>−2</sup> )	$Q_0$ (mg g <sup>−1</sup> )	$E$ (kJ mol <sup>−1</sup> )		$R^2$	
$5.0 \times 10^{-7}$	4.00	1.00		0.9465	

of coulombic forces under acid conditions of work. On this ground, to propose kiwi peels as a recyclable adsorbent material (focusing the attention on DB adsorbed from a NaCl solution), 10 cycles of adsorption and desorption were consecutively performed, choosing hot water (323 K) at pH 6 as the best condition for the desorption. Moreover, 15 minutes were

selected as the desorption contact time. Specifically, after DB adsorption from a 0.5 M NaCl solution in 60 minutes, the adsorbent was swollen in hot water for 15 minutes. The % of adsorption and desorption was thus calculated and reported in Fig. 6(C). Very interestingly, the adsorbent maintained the same efficiency without significant differences in each cycle,



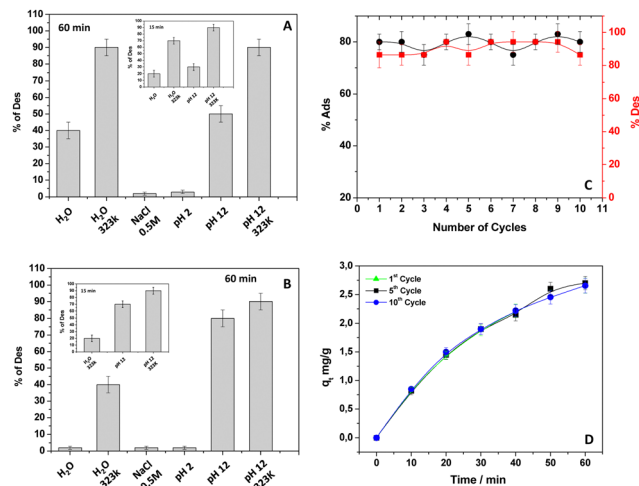


**Fig. 6** % of DB desorption from kiwi peels (calculated at 60 minutes as contact desorption time) under different conditions. The related adsorption was obtained from a solution of DB  $13 \text{ mg L}^{-1}$  and 50 mg of peels in (A) NaCl 0.5 M solution, pH 6; (B) pH 2 at room temperature. The inset in both figures shows the results obtained at 15 minutes of desorption time. (C) Consecutive cycles of DB adsorption and desorption in hot water (the % of adsorption and desorption are calculated at 60 and 15 minutes, respectively); (D) adsorption capacities  $q_t$  ( $\text{mg g}^{-1}$ ) of kiwi peels after the 1st and 10th cycle of adsorption.

highlighting the great performance of the proposed material as a low-cost and eco-friendly adsorbent for water treatment. Furthermore, the adsorption capacity of kiwi peels was also calculated after the 10th cycle of adsorption/desorption, and it was compared with the results related to the first cycle. Fig. 6(D) shows the obtained results. As can be appreciated, the  $q_t$  values at different adsorption times were practically superimposed, evidencing the great performance of kiwi peels. So, the runs could be extended up to 10 cycles for rendering this novel adsorbent, proposed to treat water from dyes, competitive with other more efficient materials, respecting the sustainability principles. Indeed, regarding the past literature, the use of hot water appeared eco-friendly because the desorption time was very low. For example, Singh *et al.*,<sup>26</sup> about the removal of Congo Red and Direct Blue-1, reported the mycosynthesized iron nanoparticle regeneration by using a 0.08 M NaOH solution for 120 min. The obtained regenerated adsorbents were further reused, and only five cycles of regeneration were performed. The recovery of Direct Red 81 adsorbed on *Argemone mexicana* was achieved again by eluting the dye in NaOH solution.<sup>29</sup> Li *et al.*<sup>30</sup> reported the Direct green 6 removal and NaOH solutions were proposed for the desorption from Y(III)-chitosan-doped fly ash composite. During the study, although 5 cycles of desorption were attempted, the reported adsorption efficiencies collapsed at increasing the runs of adsorption/desorption. Noreen *et al.*<sup>32</sup> showed the ZnO, MgO, and FeO high adsorption efficiencies for Direct sky Blue dye removal. However, also, in this case, the desorption was performed using 0.1–0.9 M NaOH<sup>32</sup> for a long contact time, at least 120 minutes with low desorption %. Moreover, always for DB removal, also Rizzi *et al.*<sup>11,12</sup> accounted for the regeneration of olive pomace

and MCM-41 nanoparticles with NaOH. Only a few cycles of adsorption/desorption were described, and in the case of MCM-41, the adsorbent appeared disrupted after 5 runs.<sup>11,12</sup> On the other hand, during this work, DB was recycled under safer experimental conditions, presenting a long-lasting material.

### ATR-FTIR analysis

Kiwi peels are mainly composed of lignin and cellulose, exposing on their surface some functional groups: alcohols, aldehydes, ketones, carboxylic, phenolic, and ether groups. The ATR-FTIR spectrum of kiwi peels is reported in Fig. S6A (ESI<sup>†</sup>) (black line). Both the inner and outer sides of peels were investigated without great differences between them in terms of ATR-FTIR spectrum features, as already described by Gubitosa *et al.*<sup>34</sup> The band at  $3307 \text{ cm}^{-1}$  was referred to as the O–H vibration from phenols, lignin, hemicellulose, and cellulose. The related asymmetric and symmetric C–H bond stretching of methyl and methylene groups were detected at  $2840$  and  $2911 \text{ cm}^{-1}$ , respectively. At  $1727 \text{ cm}^{-1}$ , the weak contribution of C=O groups from hemicellulose esters or carbonyl esters of lignin was observed. The stretching and bending vibration that arose from the hydroxyl groups of cellulose was detected at  $1614 \text{ cm}^{-1}$ . The C=O stretching vibration in the conjugated carbonyl of lignin should also be taken into account. The strong band at  $1030 \text{ cm}^{-1}$  was referred to as the –C–O–C– vibration from the skeleton of cellulose and hemicellulose. In the region  $1100$  and  $1500 \text{ cm}^{-1}$  other weak bands were observed and attributed to  $\text{CH}_3$ ,  $-\text{CH}_2-$ , and C–H moieties, besides the polyphenolic aromatic ring C=C vibration due to the presence of cellulose, hemicellulose, and lignin. The contribution of C–O vibrations in carboxylate groups, and the stretching of esters, ethers, or phenol groups, should be taken into account. The same features were observed after the DB adsorption (red curve), from a solution at pH 6 and NaCl 0.5 M, with slight changes in band position and relative intensity. The contribution of the adsorbed DB was not significantly detected (Fig. S6B, ESI<sup>†</sup> shows the ATR-FTIR signals of DB). Conversely, focusing the attention on the typical vibration bands of kiwi peels, the signal at  $1614 \text{ cm}^{-1}$  shifted to a higher wavenumber,  $1622 \text{ cm}^{-1}$ , appearing better defined, suggesting the DB coordination with cellulose OH moieties.<sup>34</sup> Accordingly, the OH signal at  $3307 \text{ cm}^{-1}$  increased its relative intensity and slightly shifted, denoting the possible formation of the H-bond with DB and the adsorbent surface, besides the OH moieties vibration contribution from DB. These observations suggested the presence of H-bonds and hydrophobic interactions between DB and the kiwi peels, as previously evidenced during the discussion. Finally, after the adsorbent recycling (green line), the IR bands' position, shape, and relative intensity appeared the same as those recorded at the beginning of the adsorption process, validating that the main adsorbent functional groups and features were not affected during the prolonged adsorption/desorption runs, as already reported by Gubitosa *et al.*<sup>34</sup> during the removal/recycling of ciprofloxacin.

### Removal of other textile dyes and their mixtures

The great performances of kiwi peels were highlighted by showing the ability to remove other textile dyes, *i.e.*, Direct

Yellow 86 (DY) and Direct Red 83:1 (DR). The experiments were performed by removing the single dyes and their mixture. Indeed, the affinity of DY and DR for kiwi peels did not appear different from the behavior exhibited by DB. Indeed, the removal of both dyes was quite complete,  $\approx 80\%$ , under the same condition of work proposed for the DB removal. Accordingly, the removal of the color mixture better evidenced the finding that could represent an important aspect of the real treatment of wastewater. For this purpose, a mixture of DR, DB, and DY in a 0.5 M NaCl solution was studied (Fig. 7(A)). The adsorption process was monitored through visible spectroscopy, as discussed before in the case of the DB removal. It is worth mentioning that each dye showed its typical visible absorption spectrum that contributes to the global visible absorption spectrum of the mixture, constituted by an envelope of absorption bands of a single dye. Specifically, DY contributes to its absorption showing a maximum of around 390 nm, DR at 550 nm, and DB at 600 nm (indicated with asterisks in Fig. 7(A)).<sup>13</sup>

The visible spectra were collected before and after the contact with the adsorbent by selecting 60 minutes as the contact time. The high efficiency of adsorption can be appreciated in Fig. 7(A). More than 50% of each pollutant was removed from the water. Interestingly, also for the mixture of the dyes, their desorption and regeneration of kiwi peels were attained. By following the same procedure to desorb DB, in Fig. 7(B), the visible spectrum of the dye-mixture after the desorption is reported. As indicated by the green circle, the DB contribution appears greater than other dyes during the desorption, as if it was preferentially desorbed with respect to DY and DR. However, the adsorbent regeneration could be considered a success, being able to desorb the three dyes even if with different efficiencies and the absence of selectivity. These results appeared very promising for the possible scale-up of the process to treat real wastewater samples. Novel horizons in treating water polluted by dyes are thus opened: kiwi peels can be

considered a low-cost and environmentally friendly adsorbent, able to adsorb different dyes and emerging pollutants without selectivity and important effects of competition, as also reported in our previous study.

### Dyeing capacity experiments of dye-kiwi peels

To explore the quality of the recycled DB from kiwi peels, dyeing experiments were performed using cotton fiber. In particular, the experiments of dyeing were achieved during the kiwi peel desorption in hot water at 323 K, without further additives, adopting 60 minutes as contact time. Fig. 8 shows the obtained results.

Fig. 8(A) and (B) show the cotton fabrics, respectively, before and after the dyeing process. Interestingly, the dyeing capacity of DB was retained after its adsorption onto kiwi peels, although the adsorbent was used for several cycles. In particular, Fig. 8(C) and (D) show the cotton fabrics colored with DB released by kiwi peels after the 5th and 10th cycles of adsorption/desorption, respectively. The obtained results are very interesting because the kiwi peels could be used directly in a dyeing batch, releasing the dye to color fibers again, lowering the associated costs. Indeed, hot water is usually required during the dyeing process.

### Preliminary information about the DB solid-state photodegradation onto kiwi peels

By adopting the same approach reported by Gubitosa *et al.*<sup>34</sup> during the photodegradation of ciprofloxacin after the adsorption onto kiwi peels, an alternative process for the adsorbent recycling was herein attempted. In general, the textile dye photodegradation in solution is well known in the literature,<sup>45–47</sup> and particularly the photoreaction of DB was

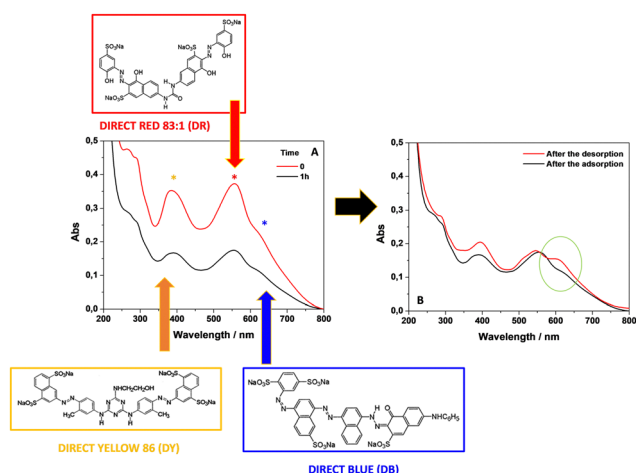


Fig. 7 Visible spectra of a mixture of DB, DR, and DY (each one at  $13 \text{ mg L}^{-1}$  in NaCl 0.5 M, pH 6 and room temperature) collected before and after 1 h of contact with kiwi peels (50 mg) (A); visible spectra of a mixture of DB, DR, and DY collected after 1 h of contact with kiwi peels, and after the desorption in hot water (desorption time 15 minutes) (B).

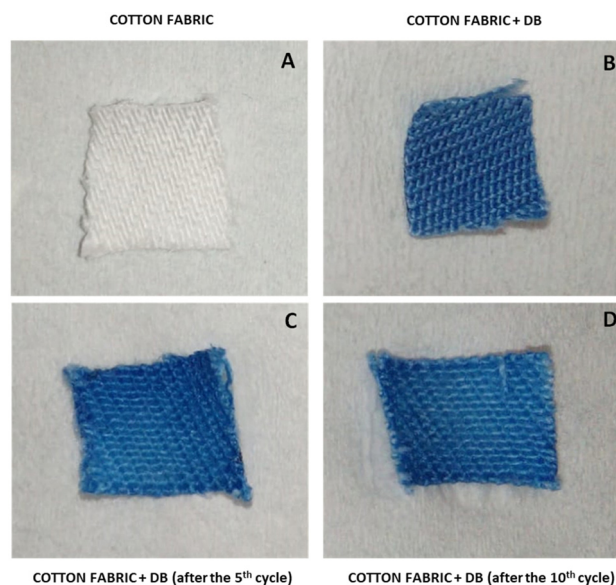


Fig. 8 Dyeing experiments of white cotton fabrics (A) with DB prior to the adsorption onto kiwi peels (B), and after the desorption from kiwi peels used 5 times (C), and 10 times (D).

studied by using AOPs, well detailing the photodegradation mechanism.<sup>46,47</sup>

Therefore, during this work, a preliminary study was carried out by proposing the use of AOPs to induce, in this case, the DB solid-state photodegradation after the adsorption onto kiwi peels. The main aim was to find the best experimental conditions for obtaining the highest DB degradation and propose an alternative adsorbent regeneration strategy. Indeed, Gubitosa *et al.*<sup>34</sup> demonstrated that the main kiwi peel features are also retained after the AOP treatments, not affecting the adsorption capacity of the material. On this basis, the attention was focused on the synergistic use of UV light, H<sub>2</sub>O<sub>2</sub>, UV-TiO<sub>2</sub>, UV/H<sub>2</sub>O<sub>2</sub>/TiO<sub>2</sub>, Fenton, and photo-Fenton conditions.<sup>45–50</sup> Indeed, in these experimental conditions, the main product is the radical  $\bullet\text{OH}$ ,<sup>3,6,8,45–47,50</sup> a very reactive and not selective species that favors the pollutants' fast degradation. Furthermore, the use of TiO<sub>2</sub>, H<sub>2</sub>O<sub>2</sub>, and Fenton reagents in the presence of UV light should promote the additional formation of  $\bullet\text{OH}$ . In detail, the experiments were performed by placing the kiwi peels after the adsorption in water (15 mL) at pH 2 under UV light irradiation. The choice of working at acidic pH was determined by considering that DB degradation is favored at low pH.<sup>46</sup> Moreover, focusing the attention on the photocatalytic action of TiO<sub>2</sub>, since an important step in the photocatalytic oxidations is the adsorption of the species onto the photocatalyst surface, under acidic conditions, the TiO<sub>2</sub> surface is positively charged, so the adsorption of negatively charged DB is further facilitated.<sup>46</sup> According to the cases reported in Fig. 9, the water solution surrounding kiwi peels was spiked with the explored oxidant's agents.

The % of photodegraded DB was evaluated through release experiments in hot water after the performed oxidative treatments. In the first step, the degradation was attempted by placing DB-loaded kiwi peels in water and irradiating with a UV lamp for 2 h (Fig. 9(A)). Only 10% of the adsorbed DB was

destroyed. After that, the loaded adsorbent was placed in a solution containing only H<sub>2</sub>O<sub>2</sub> at different concentrations (from  $5 \times 10^{-4}$  M to  $5 \times 10^{-2}$  M), both in the dark and under UV light. The absence of any degradation was detected. The use of TiO<sub>2</sub>, suspended in water, was thus considered in different amounts by adopting, again, 2 h as irradiation time (Fig. 9(A)). The best condition was observed by placing kiwi peels in a suspension containing 1 mg of TiO<sub>2</sub>, thus obtaining  $\approx 45\%$  DB's degradation (Fig. 9(A)). The further increase of TiO<sub>2</sub> amount increased the opacity of the suspension, hindering the light penetration and decreasing the hydroxyl radical formation.<sup>46</sup> So, fixing the TiO<sub>2</sub> amount at 1 mg, the effect of adding H<sub>2</sub>O<sub>2</sub> was investigated. As shown in Fig. 9(B), adding H<sub>2</sub>O<sub>2</sub> in different concentrations (ranging from  $5 \times 10^{-4}$  M to  $5 \times 10^{-2}$  M) did not improve the process, probably due to the hydroxyl radicals self-quenching in the solution surrounding kiwi peels.<sup>34</sup> Indeed, the  $\bullet\text{OH}$  quenching occurred rapidly, preventing the radicals' migration from the bulk of the solution to the adsorbent surface where DB was located.<sup>34</sup> Furthermore, the UV "filter" effect of H<sub>2</sub>O<sub>2</sub> could reduce the TiO<sub>2</sub> activation. Indeed, by increasing the H<sub>2</sub>O<sub>2</sub> amount from  $5 \times 10^{-4}$  M to  $5 \times 10^{-2}$  M, due to the H<sub>2</sub>O<sub>2</sub> photolysis, the effect of hydroxyl radical self-quenching was more pronounced, achieving only  $\approx 35\%$  of DB's degradation with 1 mg of TiO<sub>2</sub> and H<sub>2</sub>O<sub>2</sub>  $1 \times 10^{-3}$  M. The latter condition was also explored by increasing the TiO<sub>2</sub> amount from 1 mg to 2 mg, not improving the DB degradation process that remained at  $\approx 45\%$ . Subsequently, the photo-Fenton reagent was used (Fig. 9(C)). Experiments were performed under UV light irradiation for 2 h using different amounts of H<sub>2</sub>O<sub>2</sub>, fixing the concentration of Fe<sup>2+</sup> at  $5 \times 10^{-6}$  M. Under these conditions, the DB's degradation was not high (from  $\approx 10\%$  to  $20\%$ ), and the increase of H<sub>2</sub>O<sub>2</sub> concentration (or [Fe<sup>2+</sup>]) did not improve the results. These findings could be explained, once again, considering that the self-quenching of hydroxyl radicals is the preferred process in solution. Indeed, by increasing the amount of H<sub>2</sub>O<sub>2</sub>, the effect was more pronounced. The same experiments were performed in the dark, without significant DB degradation. The addition of TiO<sub>2</sub> (1 mg) was also attempted under photo-Fenton conditions, and for example, when using H<sub>2</sub>O<sub>2</sub>  $1 \times 10^{-3}$  M and 1 mg of TiO<sub>2</sub>, the  $\approx 15\%$  of DB was degraded, not enhancing the process (Fig. 9(C)).

As a general result, the discussed strategies cannot be considered useful for solid-state degradation of the dye because they do not improve the result obtained from the use of simple TiO<sub>2</sub>, which could be considered the best condition investigated. So, fixing the TiO<sub>2</sub> amount at 1 mg, further experiments were performed by irradiating kiwi peels with UV light and increasing the irradiation time (Fig. 9(D)). The increase in irradiation time significantly improved the DB degradation observing  $\approx 30\%$ ,  $45\%$ ,  $65\%$ , and  $75\%$  after 1 h, 2 h, 4 h, and 8 h, respectively. So, the photocatalytic process could be used in synergy or as a potential alternative to the main approach discussed that proposes the DB's desorption.

In this regard, some experiments were performed to investigate if the adsorption capacity of kiwi peels changes after

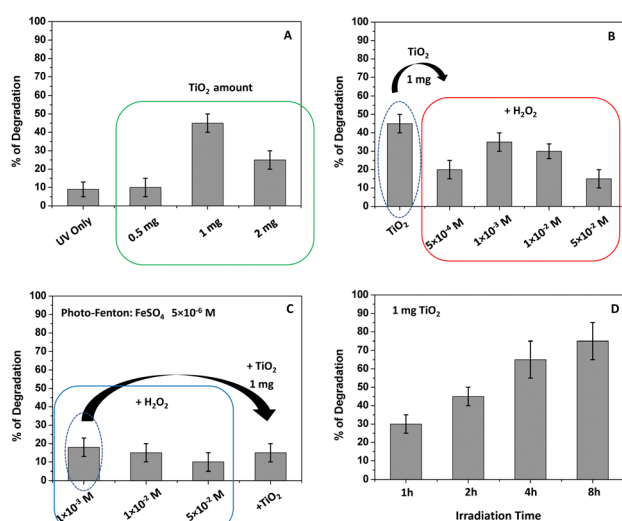


Fig. 9 % of DB photodegradation under different working conditions at pH 2. Effect of: UV light, TiO<sub>2</sub> amount (A); TiO<sub>2</sub> + H<sub>2</sub>O<sub>2</sub> (B); photo-Fenton conditions (C); UV light irradiation time on TiO<sub>2</sub> (D).

using UV light and  $\text{TiO}_2$ , or if it remains the same as that observed previous to the treatment. In accordance with what was reported by Gubitosa *et al.*,<sup>34</sup> the use of  $\text{TiO}_2$  and UV light did not affect the main chemical and morphological features of kiwi peels.

## Experimental

### Chemicals

The used kiwi fruits were obtained from local providers in Bari, South of Italy. Direct Blue 78 (molecular formula:  $\text{C}_{42}\text{H}_{25}\text{N}_7\text{Na}_4\text{O}_{13}\text{S}_4$ , molecular weight:  $1055.91 \text{ g mol}^{-1}$ , CAS Registry Number: 2503-73-3) was received from Colorprint Fashion, SL, and used without further purification. All the used chemicals were purchased from Sigma Aldrich (Milan, Italy). The pollutant stock solution,  $50 \text{ mg L}^{-1}$ , was obtained in deionized water, and it was diluted to obtain solutions having concentrations of 25, 16, 13, and  $8 \text{ mg L}^{-1}$ . HCl and NaOH solutions were used to modify the pH of the DB solutions. NaCl, LiCl, KCl,  $\text{MgCl}_2$ ,  $\text{CaCl}_2$ , NaBr, and  $\text{NaClO}_4$  were investigated to assess the role of ionic strength during the dye removal. All the analyses were performed in triplicate, and standard deviations were calculated and reported as error bands.

### Adsorbent preparation

The obtained kiwi fruits were washed well and peeled. The peels (80 mg) were placed in hot water (500 mL) under vigorous stirring for 15 minutes. If necessary, the remaining fruit pulp was mechanically removed. The process of washing was subsequently repeated three times. The obtained peels were dried in oven until reaching a constant weight and used as an adsorbent material.

### UV-visible absorption measurements

The Varian CARY 5 UV-Vis-NIR spectrophotometer (Varian Inc., now Agilent Technologies Inc., Santa Clara, CA, USA) was employed to collect the visible absorption spectra of DB in a range of 250–800 nm, at a  $1 \text{ nm s}^{-1}$  scan rate. The DB concentration was derived from the Lambert–Beer law, measuring the absorbance intensity at  $\lambda = 600 \text{ nm}$ , and adopting a molar absorption coefficient ( $\epsilon$ ) of  $20\,901 \text{ L mol}^{-1} \text{ cm}^{-1}$ .

### ATR-FTIR spectroscopy measurements

The ATR-FTIR spectra of kiwi peels before and after the pollutant adsorption/desorption were recorded in a  $4000\text{--}400 \text{ cm}^{-1}$  range using a Fourier Transform Infrared spectrometer (FTIR Spectrum Two from PerkinElmer, Waltham, MA, USA). The resolution was set at  $4 \text{ cm}^{-1}$ , and 16 scans were obtained and summed for each acquisition.

### In batch equilibrium experiments

The % of DB adsorption (% of Ads) was calculated by adopting eqn (1).<sup>34</sup>

$$\% \text{ of Ads} = \frac{A_0 - A_t}{A_0} \times 100 \quad (1)$$

where  $A_0$  and  $A_t$  are the visible absorbance intensity of the DB solution, measured at  $\lambda = 600 \text{ nm}$ , at time  $t_0$  and  $t$  time, respectively.

The adsorption capacities,  $q_t$  ( $\text{mg g}^{-1}$ ), for kiwi peels were calculated by applying eqn (2) to the experimental data.<sup>2,11,13,15,34</sup>

$$q_t = \frac{C_0 - C_t}{W} \times V \quad (2)$$

where  $V$  represents the DB solution volume (herein 15 mL),  $W$  is the dried adsorbent amount (g), and  $C_0$  and  $C_t$  are the DB concentrations, expressed as  $\text{mg L}^{-1}$ , at time  $t_0$  and  $t$  time, respectively.

50 mg of adsorbent was swelled into 15 mL of water in the presence of DB having different initial concentrations (from  $25 \text{ mg L}^{-1}$  to  $8 \text{ mg L}^{-1}$ ) at pH 6, to assess the DB amount role during the adsorption onto the kiwi peel surface. On the other hand, the adsorbent amount role was investigated by changing the weight of peels from 12 to 80 mg, in the presence of DB  $13 \text{ mg L}^{-1}$ , pH 6. The process was studied with constant stirring at room temperature (298 K). The solution's ionic strength was changed by using different salts after fixing the amount of the adsorbate and adsorbent (50 mg of kiwi peels, and  $13 \text{ mg L}^{-1}$  of DB). NaCl was adopted to infer the role of salt concentrations. The pH values, ranging from 2 to 12, and temperature values, from 275 to 333 K, were also changed during the adsorption.

### Adsorption kinetics

The pseudo-first-order (PFO) and pseudo-second-order (PSO) kinetic models were applied to the experimental data. For this purpose, eqn (3) and (4) were used to describe PFO and PSO models, respectively.<sup>2,11,13,15,34</sup>

$$\ln(q_e - q_t) = \ln(q_e) - K_1 \times t \quad (3)$$

$$\frac{t}{q_t} = \frac{1}{K_2 q_e^2} + \frac{1}{q_e} \times t \quad (4)$$

where  $q_e$  ( $\text{mg L}^{-1}$ ) represents the kiwi peels' adsorption capacities at equilibrium, and  $q_t$  ( $\text{mg L}^{-1}$ ) is the adsorption capacity at time  $t$ .  $k_1$  ( $\text{min}^{-1}$ ) and  $k_2$  ( $\text{g (mg min)}^{-1}$ ) are the rate constants of PFO and PSO models, respectively.

Eqn (5) was also used to infer the intraparticle diffusion role described by the Weber–Morris equation.<sup>34</sup>

$$q_t = k_{\text{int}} \times t^{1/2} + C \quad (5)$$

In this case,  $k_{\text{int}}$  represents the kinetic constant expressed in  $\text{mg (g}^{-1} \text{ min}^{-1/2})$ , referred to as the intra-particle diffusion rate, and  $C$  is the thickness of the boundary layer.

### Thermodynamic studies

For this purpose, different temperature values ranging from 275 to 333 K were adopted. So, the free energy ( $\Delta G^\circ$ ), entropy ( $\Delta S^\circ$ ), and enthalpy ( $\Delta H^\circ$ ) were calculated for the DB adsorption. In particular, eqn (6) was used to calculate the free energy.<sup>29,30,34</sup>

$$\Delta G^\circ = -RT \ln K_{\text{eq}} \quad (6)$$



where  $R = 8.314 \text{ J mol}^{-1} \text{ K}^{-1}$ ,  $T$  is the temperature (K), and  $K_{\text{eq}}$  is the equilibrium constant ( $q_e/C_e$ ).  $\Delta H^\circ$  and  $\Delta S^\circ$  were obtained by using eqn (7).

$$\ln K_{\text{eq}} = -\frac{\Delta H^\circ}{RT} + \frac{\Delta S^\circ}{R} \quad (7)$$

### Adsorption isotherms

The adopted isotherms of adsorption were the following: Langmuir, Freundlich, Temkin, and Dubinin–Radushkevich.<sup>29–32,34</sup> The Langmuir model could be herein applied and well fit the adsorption process if all the adsorption sites are characterized by constant energy during the DB adsorption. Furthermore, a monolayer of dye can be supposed to be adsorbed on the surface of kiwi peels without strong interactions between the molecules of DB. Eqn (8) was applied to describe the Langmuir model.<sup>34</sup>

$$\frac{C_e}{q_e} = \frac{1}{K_L Q_0} + \frac{C_e}{Q_0} \quad (8)$$

In eqn (8),  $q_e$  ( $\text{mg g}^{-1}$ ) is the pollutant adsorbed amount at equilibrium,  $C_e$  is the correspondent equilibrium concentration in solution expressed in  $\text{mg L}^{-1}$ ,  $K_L$  represents the Langmuir equilibrium constant ( $\text{L mg}^{-1}$ ), and  $Q_0$  is the adsorbent maximum adsorption capacity ( $\text{mg g}^{-1}$ ) value.<sup>34</sup>

The Freundlich isotherm, if fitted with the experimental data, should reflect the DB adsorption onto a heterogeneous surface with adsorption sites having different energies as a function of the surface coverage. In this case, the heat of adsorption should decrease exponentially during the DB removal. Eqn (9) describes the Freundlich model.<sup>34</sup>

$$\log(q_e) = \log(K_F) + \frac{1}{n} \log(C_e) \quad (9)$$

$K_F$  ( $\text{L mg}^{-1}$ ) is the Freundlich constant, and  $n$  represents the heterogeneity factor. The  $1/n$  value can assume different values: if the adsorption process is irreversible,  $1/n = 0$ , favorable,  $0 < 1/n < 1$ , and unfavorable,  $1/n > 1$ .<sup>34</sup>

The Temkin model describes the influence of the adsorbate–adsorbent interactions on the adsorption energy. This isotherm suggests that the heat of adsorption should decrease linearly during the DB removal due to adsorbent/adsorbate interactions. Eqn (10) was applied to use the Temkin model.<sup>34</sup>

$$q_e = B_1 \ln(K_T) + B_1 \ln(C_e) \quad (10)$$

$K_T$  ( $\text{L mol}^{-1}$ ) is the equilibrium binding constant, and  $B_1$  is related to the heat of adsorption.

The Dubinin–Radushkevich isotherm (D–R) model was also employed by applying eqn (11). In this case, the model assumes the adsorption onto a heterogeneous surface in which a Gaussian energy distribution can be used.<sup>34</sup>

$$\ln q_e = \ln(Q_0) - K_{D-R} \times \varepsilon^2 \quad (11)$$

$q_e$  ( $\text{mg g}^{-1}$ ) is the equilibrium adsorption capacity,  $Q_0$  ( $\text{mg g}^{-1}$ ) is the theoretical maximum adsorption capacity, and  $K_{D-R}$

( $\text{mol}^2 \text{ J}^{-2}$ ) is the Dubinin–Radushkevich isotherm constant.  $\varepsilon$  is the potential of Polanyi, and it is described by eqn (12).

$$\varepsilon = RT \ln \left( 1 + \frac{1}{C_e} \right) \quad (12)$$

$R$  is the gas constant ( $8.314 \text{ J mol}^{-1} \text{ K}^{-1}$ ),  $T$  is the absolute temperature (K), and  $C_e$  represents the DB equilibrium concentration ( $\text{mg L}^{-1}$ ).

It is worth mentioning that this model can distinguish between physical and chemical adsorption by calculating the value of energy,  $E$ , by using eqn (13).

$$E = \frac{1}{\sqrt{2K_{D-R}}} \quad (13)$$

If the output value of  $E$  is in the range of 8–16  $\text{kJ mol}^{-1}$ , the chemisorption should be considered during the adsorption process; conversely, for  $E < 8 \text{ kJ mol}^{-1}$ , the physisorption should be more important.<sup>28,34</sup>

### In batch desorption experiments

Desorption experiments were performed by using different conditions of work. However, hot distilled water at 323 K was proposed (adopted volume of 15 mL) to perform 10 cycles of DB adsorption and desorption. Visible absorption spectroscopy was used to infer the amount of desorbed DB.

### Kiwi peel point of zero charge determination

The pH at which the kiwi peel point of zero charge occurred ( $\text{pH}_{\text{PZC}}$ ) was calculated by following the procedure adopted by Gubitosa *et al.*<sup>34</sup> In detail, 30 mL of a  $5.0 \times 10^{-2} \text{ M}$  NaCl solution was prepared after changing the pH values from 2 to 12 ( $\text{pH}_i$ ) by using HCl and NaOH. So, the pH of solutions was measured before ( $\text{pH}_i$ ) and after ( $\text{pH}_F$ ) swelling 50 mg of the kiwi peels for 48 h, under continuous stirring. The  $\text{pH}_{\text{PZC}}$  value was obtained by plotting  $\text{pH}_i$  versus  $\text{pH}_i$  and  $\text{pH}_i$  versus  $\text{pH}_F$ ; the intersection of these lines represents the  $\text{pH}_{\text{PZC}}$  value.

### Photodegradation of Direct Blue 78

The solid-state photodegradation of DB was obtained after its removal from water using AOPs. A UV lamp (UV fluorescent lamp, Spectroline, Model CNF 280C/FE,  $\lambda$  254 nm, light flux  $0.2 \text{ mW cm}^{-2}$ ; USA) was employed to irradiate the adsorbent placed in water (15 mL) by adopting several conditions of work detailed in the paper. The irradiation was performed on solutions under continuous stirring. Commercial Evonik Aerioxide  $\text{TiO}_2$  P25 (formerly Degussa P25),  $\text{FeSO}_4$   $1 \times 10^{-3} \text{ M}$ , and commercial  $\text{H}_2\text{O}_2$  (30%) were used during the experiments.

## Conclusions

This work proposes kiwi peels' wastes as a resource for the textile dye removal from wastewater. DB was adopted as a model textile dye, evidencing the main chemical and physical features of the whole adsorption process. The removal occurred both under acidic working conditions and/or in the presence of salts at neutral pH values. If during the former experimental

conditions, the presence of an electrostatic interaction between DB and the adsorbent was important, in the latter one, the contribution of hydrophobic interactions and the presence of H-bonds predominated. In particular, focusing first on the pollutant removal in the absence of salts, it occurred high at pH values 2 and 3 and decreased by increasing the pH values. The DB removal was blocked up to pH 4. The results agree with the DB's  $pK_a < 2$  for  $SO_3^-$  moieties and the PZC of the adsorbent ( $pH_{PZC} = 4$ ). At pH 2, the  $-SO_3^-$  groups of DB were deprotonated and negatively charged; on the other hand, the kiwi peel surface was positive. The attraction predominates. After pH 4, the kiwi peels acquired a net negative charge, and the DB was still negative, so the repulsion occurred. When the DB adsorption was carried out in the presence of salt, *i.e.*, NaCl, the process was salt-amount dependent, and by increasing the concentration of NaCl from 0.01 M to 1 M, the DB removal results were enhanced. The presence of a hydrophobic interaction was confirmed by FTIR-ATR analysis, which also evidenced the contribution of H-bonds. To avoid hard working conditions, the main focus was on the adsorption process in the presence of electrolytes. As suggested by the thermodynamic parameters, the process was spontaneous ( $\Delta G^\circ < 0$ ), and endothermic ( $\Delta H^\circ > 0$ ), showing an increase in entropy during the process. The isotherms and the kinetics were studied, and the adsorption process was well described by all the proposed isotherm models, showing a very good correlation with the Freundlich equation. The pseudo-first and second-order kinetic models described DB adsorption as a multi-step process where both the inner and external DB diffusion acquire kinetic relevance. Accordingly, it was observed that the kiwi peel adsorption capacities increased by increasing the adsorbent and pollutant amount, suggesting the important role of free active sites on the peel surface and DB diffusion during the adsorption. Finally, using eco-friendly approaches, pollutant desorption was investigated for favoring the recycling of both DB and kiwi peels. For this purpose, hot water was selected, and 10 cycles of adsorption/desorption were performed, increasing the adsorbent lifetime, according to Green Chemistry and Circular Economy principles. Furthermore, besides the recycling of the adsorbent, DB recycling was also demonstrated, proposing qualitatively cotton fabric dyeing by using the desorbed DB. So, kiwi peels appeared as a powerful candidate as potential adsorbents to clean wastewater containing textile dyes. Indeed, adsorption experiments were also performed in the presence of dye mixtures, *i.e.*, DB, DR, and DY, evidencing the possibility of removing the pollutants even in this case. Finally, preliminary experiments related to the solid-state DB photodegradation were attempted as an alternative to its recycling, by exploiting AOPs. More specifically, the use of  $TiO_2$  and UV light occurred as the best working condition to obtain the highest DB degradation that was time-dependent. The adsorption capacity of kiwi peels was again studied after the UV light treatment, resulting in not being affected by the photocatalytic treatment. The opportunity to adopt this alternative strategy for adsorbent regeneration was thus achieved and proposed.

## Author contributions

Vito Rizzi: conceptualization, investigation, validation, methodology, writing – review, and editing; Jennifer Gubitosa: conceptualization, validation, investigation, writing – original draft preparation; Paola Fini: investigation, validation, data curation; Sergio Nuzzo: visualization, imaging elaboration; Pinalysa Cosma: formal analysis, resources, project administration, writing – review and editing, funding acquisition.

## Conflicts of interest

There are no conflicts to declare.

## Acknowledgements

This work was supported by the following projects: “Research for Innovation (REFIN) per l'individuazione dei progetti di ricerca” – PUGLIA FESR-FSE 2014/2020, Project title: “Incontro tra Ricerca & Impresa per lo Sviluppo Sostenibile del territorio (IRISS): valorizzazione di scarti alimentari per la rimozione di contaminanti emergenti dalle acque”; “Dottorati di ricerca in Puglia XXXIII, XXXIV, XXXV ciclo, POR PUGLIA FESR-FSE 2014/2020”; Horizon Europe Seeds, Project title: “Gestione sostenibile di scarti Agroalimentari come fonte Innovativa di biomateriali multifunzionali per la salute umana e l'Ambiente (G.A.I.A.)”.

## Notes and references

- 1 I. B. Obinna and Enyoh Ebere, A review: Water pollution by heavy metal and organic pollutants: Brief review of sources, effects and progress on remediation with aquatic plants, *Anal. Methods Environ. Chem. J.*, 2019, 2(3), 5–38.
- 2 V. Rizzi, J. Gubitosa, P. Fini, S. Nuzzo and P. Cosma, Amino-grafted mesoporous MCM-41 and SBA-15 recyclable adsorbents: Desert-rose-petals-like SBA-15 type as the most efficient to remove azo textile dyes and their mixture from water, *Sustainable Mater. Technol.*, 2020, 26, e00231.
- 3 V. Rizzi, J. Gubitosa, P. Fini, R. Romita, A. Agostiano, S. Nuzzo and P. Cosma, Commercial bentonite clay as low-cost and recyclable “natural” adsorbent for the Carbazim removal/recover from water: Overview on the adsorption process and preliminary photodegradation considerations, *Colloids Surf., A*, 2020, 602, 125060.
- 4 V. Rizzi, J. Gubitosa, P. Fini, A. Petrella, R. Romita, A. Agostiano and P. Cosma, A “classic” material for capture and detoxification of emergent contaminants for water purification: The case of tetracycline, *Environ. Technol. Innovation*, 2020, 19, 100812.
- 5 V. Rizzi, J. Gubitosa, P. Fini, R. Romita, S. Nuzzo and P. Cosma, Chitosan Biopolymer from Crab Shell as Recyclable Film to Remove/Recover in Batch Ketoprofen from Water: Understanding the Factors Affecting the Adsorption Process, *Materials*, 2019, 12, 3810.

- 6 V. Rizzi, F. Romanazzi, J. Gubitosa, P. Fini, R. Romita, A. Agostiano, A. Petrella and P. Cosma, Chitosan Film as Eco-Friendly and Recyclable Bio-Adsorbent to Remove/Recover Diclofenac, Ketoprofen, and their Mixture from Wastewater, *Biomolecules*, 2019, **9**, 571.
- 7 R. Romita, V. Rizzi, P. Semeraro, J. Gubitosa, J. A. Gabaldón, M. I. F. Gorbe, V. M. G. López, P. Cosma and P. Fini, Operational parameters affecting the atrazine removal from water by using cyclodextrin based polymers as efficient adsorbents for cleaner technologies, *Environ. Technol. Innovation*, 2019, **16**, 100454.
- 8 V. Rizzi, D. Lacalamita, J. Gubitosa, P. Fini, A. Petrella, R. Romita, A. Agostiano, J. A. J. A. Gabaldón, M. I. M. I. Fortea Gorbe, T. Gómez-Morte and P. Cosma, Removal of tetracycline from polluted water by chitosan-olive pomace adsorbing films, *Sci. Total Environ.*, 2019, **693**, 133620.
- 9 V. Rizzi, C. Mongiovi, P. Fini, A. Petrella, P. Semeraro and P. Cosma, Operational parameters affecting the removal and recycling of direct blue industrial dye from wastewater using bleached oil mill waste as alternative adsorbent material, *Int. J. Environ. Agric. Biotechnol.*, 2017, **2**, 1560–1572.
- 10 A. Petrella, D. Spasiano, V. Rizzi, P. Cosma, M. Race and N. De Vietro, Thermodynamic and kinetic investigation of heavy metals sorption in packed bed columns by recycled lignocellulosic materials from olive oil production, *Chem. Eng. Commun.*, 2019, **206**, 1715–1730.
- 11 V. Rizzi, E. A. Prasetyanto, P. Chen, J. Gubitosa, P. Fini, A. Agostiano, L. De Cola and P. Cosma, Amino grafted MCM-41 as highly efficient and reversible ecofriendly adsorbent material for the Direct Blue removal from wastewater, *J. Mol. Liq.*, 2019, **273**, 435–446.
- 12 V. Rizzi, F. Fiorini, G. Lamanna, J. Gubitosa, E. A. Prasetyanto, P. Fini, F. Fanelli, A. Nacci, L. De Cola and P. Cosma, Polyamidoamine-Based Hydrogel for Removal of Blue and Red Dyes from Wastewater, *Adv. Sustainable Syst.*, 2018, **2**, 1700146.
- 13 V. Rizzi, A. Longo, T. Placido, P. Fini, J. Gubitosa, T. Sibillano, C. Giannini, P. Semeraro, E. Franco, M. Ferrandiz and P. Cosma, A comprehensive investigation of dye–chitosan blended films for green chemistry applications, *J. Appl. Polym. Sci.*, 2017, **135**, 45945.
- 14 V. Rizzi, F. D'Agostino, J. Gubitosa, P. Fini, A. Petrella, A. Agostiano, P. Semeraro and P. Cosma, An Alternative Use of Olive Pomace as a Wide-Ranging Bioremediation Strategy to Adsorb and Recover Disperse Orange and Disperse Red Industrial Dyes from Wastewater, *Separations*, 2017, **4**(4), 29.
- 15 V. Rizzi, F. D'Agostino, P. Fini, P. Semeraro and P. Cosma, An interesting environmental friendly cleanup: The excellent potential of olive pomace for disperse blue adsorption/desorption from wastewater, *Dyes Pigm.*, 2017, **140**, 480–490.
- 16 V. Rizzi, J. Gubitosa, R. Signorile, P. Fini, C. Ceccone, A. Matencio, F. Trotta and P. Cosma, Cyclodextrin nanosponges as adsorbent material to remove hazardous pollutants from water: The case of ciprofloxacin, *Chem. Eng. J.*, 2021, **411**, 128514.
- 17 V. Rizzi, J. Gubitosa, P. Fini, R. Romita, S. Nuzzo, J. A. Gabaldón, M. I. F. Gorbe, T. Gómez-Morte and P. Cosma, Chitosan film as recyclable adsorbent membrane to remove/recover hazardous pharmaceutical pollutants from water: the case of the emerging pollutant Furosemide, *J. Environ. Sci. Health, Part A: Toxic/Hazard. Subst. Environ. Eng.*, 2021, **56**, 145–156.
- 18 A. Murcia-Salvador, J. A. Pellicer, M. I. Fortea, V. M. Gómez-López, M. I. Rodríguez-López, E. Núñez-Delicado and J. A. Gabaldón, *Polymer*, 2019, 11.
- 19 D. D'Amato and J. Korhonen, Integrating the green economy, circular economy and bioeconomy in a strategic sustainability framework, *Ecol. Econ.*, 2021, **188**, 107143.
- 20 M. Li, D. Gao, S. Cui, Y. Shi and N. Liu, Fabrication of Fe<sub>3</sub>O<sub>4</sub>/ZIF-67 composite for removal of direct blue 80 from water, *Water Environ. Res.*, 2020, **92**, 740–748.
- 21 M. H. Marzbali, A. Mir, M. Pazoki, R. Pourjamshidian and M. Tabeshnia, Removal of direct yellow 12 from aqueous solution by adsorption onto spirulina algae as a high-efficiency adsorbent, *J. Environ. Chem. Eng.*, 2017, **5**, 1946–1956.
- 22 A. Bhatnagar, E. Kumar, A. K. Minocha, B.-H. Jeon, H. Song and Y.-C. Seo, Removal of Anionic Dyes from Water using Citrus limonum (Lemon) Peel: Equilibrium Studies and Kinetic Modeling, *Sep. Sci. Technol.*, 2009, **44**, 316–334.
- 23 V. S. Munagapati, V. Yarramuthi, Y. Kim, K. M. Lee and D. S. Kim, Removal of anionic dyes (Reactive Black 5 and Congo Red) from aqueous solutions using Banana Peel Powder as an adsorbent, *Ecotoxicol. Environ. Saf.*, 2018, **148**, 601–607.
- 24 D. Sun, X. Zhang, Y. Wu and X. Liu, Adsorption of anionic dyes from aqueous solution on fly ash, *J. Hazard. Mater.*, 2010, **181**, 335–342.
- 25 R. Jiang, G. Yu, P. Ndagijimana, Y. Wang, F. You, Z. Xing and Y. Wang, Effective adsorption of Direct Red 23 by sludge biochar-based adsorbent: adsorption kinetics, thermodynamics and mechanisms study, *Water Sci. Technol.*, 2021, **83**, 2424–2436.
- 26 G. Singh, V. Kumar and S. K. Dwivedi, Comparative Investigation of Congo Red and Direct Blue-1 Adsorption on Mycosynthesized Iron Nanoparticle, *J. Clust. Sci.*, 2022, **33**, 1889–1905.
- 27 T. El Malah, H. F. Nour, E. K. Radwan, R. E. Abdel Mageid, T. A. Khatatb and M. A. Olson, A bipyridinium-based polyhydrazone adsorbent that exhibits ultrahigh adsorption capacity for the anionic azo dye, direct blue 71, *Chem. Eng. J.*, 2021, **409**, 128195.
- 28 A. Alhujaily, H. Yu, X. Zhang and F. Ma, Adsorptive removal of anionic dyes from aqueous solutions using spent mushroom waste, *Appl. Water Sci.*, 2020, **10**, 183.
- 29 S. Khamparia and D. Jaspal, Adsorptive removal of Direct Red 81 dye from aqueous solution onto Argemone mexicana, *Sustainable Environ. Res.*, 2016, **26**, 117–123.
- 30 B. Li and Z. Ren, Superior Adsorption of Direct Dye from Aqueous Solution by Y(III)-Chitosan-Doped Fly Ash Composite as Low-Cost Adsorbent, *J. Polym. Environ.*, 2020, **28**, 1811–1821.

- 31 E. A. Alabbad, Efficacy assessment of natural zeolite containing wastewater on the adsorption behaviour of Direct Yellow 50 from; equilibrium, kinetics and thermodynamic studies, *Arabian J. Chem.*, 2021, **14**, 103041.
- 32 S. Noreen, U. Khalid, S. M. Ibrahim, T. Javed, A. Ghani, S. Naz and M. Iqbal, ZnO, MgO and FeO adsorption efficiencies for direct sky Blue dye: Equilibrium, kinetics and thermodynamics studies, *J. Mater. Res. Technol.*, 2020, **9**, 5881–5893.
- 33 A. Bhatnagar, M. Sillanpää and A. Witek-Krowiak, Agricultural waste peels as versatile biomass for water purification – A review, *Chem. Eng. J.*, 2015, **270**, 244–271.
- 34 J. Gubitosa, V. Rizzi, D. Cignolo, P. Fini, F. Fanelli and P. Cosma, From agricultural wastes to a resource: Kiwi Peels, as long-lasting, recyclable adsorbent, to remove emerging pollutants from water. The case of Ciprofloxacin removal, *Sustainable Chem. Pharm.*, 2022, **29**, 100749.
- 35 J. Gubitosa, V. Rizzi, P. Fini, S. Nuzzo and P. Cosma, *Process.*, 2022, **10**.
- 36 S. Alkan, A. rıza Kul and A. Yagiz, Adsorption of textile dyes from aqueous solutions by using kiwifruit (Ordu) peel, *Fresenius Environ. Bull.*, 2017, **26**, 7045–7053.
- 37 K. M. Al-Qahtani, Water purification using different waste fruit cortexes for the removal of heavy metals, *J. Taibah Univ. Sci.*, 2016, **10**, 700–708.
- 38 L. A. Mokif, N. A. Abdulhusain and S. O. H. AL-Mamoori, The Possibility of Using the kiwi Peels as an Adsorbent for Removing Nitrate from Water, *J. Univ. Babylon Eng. Sci.*, 2018, **26**, 192–197.
- 39 A. Saleh Jafer and A. A. Hassan, *J. Phys.: Conf. Ser.*, 2019, **1294**, 072013.
- 40 M. Rahimnejad, K. Pirzadeh, I. Mahdavi and S. M. Peyghambarzadeh, Pb(II) removal from aqueous solution by adsorption on activated carbon from kiwi peel, *Environ. Eng. Manag. J.*, 2018, **17**, 1293–1300.
- 41 J. Wang, Y. Zhou, X. Liu, Q. Liu, M. Hao, S. Wang, Z. Chen, H. Yang and X. Wang, Design and application of metal-organic framework membranes for gas and liquid separations, *Sep. Purif. Technol.*, 2024, **329**, 125178.
- 42 S. Dhaka, R. Kumar, A. Deep, M. B. Kurade, S. W. Ji and B. H. Jeon, Metal-organic frameworks (MOFs) for the removal of emerging contaminants from aquatic environments, *Coord. Chem. Rev.*, 2019, **380**, 330–352.
- 43 S. Endo, A. Pfennigsdorff and K. U. Gos, Salting-Out Effect in Aqueous NaCl Solutions: Trends with Size and Polarity of Solute Molecules, *Environ. Sci. Technol.*, 2012, **46**, 1496–1503.
- 44 S. M. Burkinshaw, The role of inorganic electrolyte (salt) in cellulosic fibre dyeing: Part 2 theories of how inorganic electrolyte promotes dye uptake, *Color. Technol.*, 2021, **137**, 547–586.
- 45 A. Serrano-Martínez, M. T. Mercader-Ros, I. Martínez-Alcalá, C. Lucas-Abellán, J. A. Gabaldón and V. M. Gómez-López, Degradation and toxicity evaluation of azo dye Direct red 83:1 by an advanced oxidation process driven by pulsed light, *J. Water Process Eng.*, 2020, **37**, 101530.
- 46 Y. Song, J. Li and B. Bai, TiO<sub>2</sub>-Assisted Photodegradation of Direct Blue 78 in Aqueous Solution in Sunlight, *Water, Air, Soil Pollut.*, 2010, **213**, 311–317.
- 47 D. Marković, B. Jokić, Z. Šaponjić, B. Potkonjak, P. Jovančić and M. Radetić, Photocatalytic Degradation of Dye C.I. Direct Blue 78 Using TiO<sub>2</sub> Nanoparticles Immobilized on Recycled Wool-Based Nonwoven Material, *Clean: Soil, Air, Water*, 2013, **41**, 1002–1009.
- 48 V. Rizzi, I. Losito, A. Ventrella, P. Fini, A. Fraix, S. Sortino, A. Agostiano, F. Longobardi and P. Cosma, Rose Bengal-photosensitized oxidation of 4-thiothymidine in aqueous medium: evidence for the reaction of the nucleoside with singlet state oxygen, *Phys. Chem. Chem. Phys.*, 2015, **17**, 26307–26319.
- 49 V. Rizzi, I. Losito, R. Abbattista, P. Fini, A. Agostiano, T. R. I. Cataldi and P. Cosma, Potential of 4-thiothymidine as a molecular probe for H<sub>2</sub>O<sub>2</sub> in systems related to Photo-Dynamic therapy: A structuristic and mechanistic insight by UV-visible and FTIR-ATR spectroscopies and by Electro-Spray ionization mass spectrometry, *J. Mol. Liq.*, 2018, **264**, 398–409.
- 50 V. Rizzi, P. Cosma, R. Abbattista, P. Fini, A. Agostiano, T. R. I. Cataldi and I. Losito, Reactivity of 4-thiothymidine with Fenton reagent investigated by UV-visible spectroscopy and electrospray ionization mass spectrometry, *J. Mass Spectrom.*, 2019, **54**, 389–401.